

DC and AC Performance of InGaZnO Thin-Film Transistors on Flexible PEEK Substrate

Qazi Zahid Husain, Dianne Corsino, Federica Catania, Koichi Ishida, Tilo Meister, *Member, IEEE*, Frank Ellinger, *Senior Member, IEEE*, Niko Münzenrieder, *Senior Member, IEEE*, and Giuseppe Cantarella, *Member, IEEE*

Abstract—Thin-Film Transistors (TFTs) play a vital role in flexible electronics. Here, vacuum-processed amorphous Indium–Gallium–Zinc–Oxide-based TFTs are fabricated on a 50 μm thick polyetheretherketone (PEEK) flexible substrate. The AC and DC performances of TFTs with channel length down to 3 μm are studied. The devices exhibit effective mobility, threshold voltage, and on/off current ratio 19.6 $\text{cm}^2 \text{V}^{-1} \text{s}^{-1}$, 2.9 V, and 3×10^{10} , respectively. To address device stability, bias stress tests are performed, resulting in the maximum variation in the threshold voltage of +0.3 V and –0.6 V for a gate voltage stress of +5 V and –5 V, respectively, applied for 10 min. The AC performances of IGZO-based TFT on this substrate are reported for the first time. Here, the measured unity gain current frequency and unity gain power frequency are 5.4 MHz and 28.5 MHz. Additionally, the TFTs stay fully functional when bent to radii as small as 3 mm exhibiting only minor mobility and threshold voltage variations of +0.4% and –0.2 V. After a dynamic bending test up to 5000 cycles, the mobility and threshold voltage of the TFT deviate by +12.9% and +0.2 V, respectively. These results demonstrate that biocompatible PEEK is a potential substrate for the realization of future unobtrusive wearable systems.

Index Terms—Flexible electronics, Indium-gallium-zinc-oxide, Polyetheretherketone, Thin-film transistors.

I. INTRODUCTION

STARTING from the demonstration of first flexible transistors in the 1960s [1], the field of flexible electronics has rapidly expanded. This has been driven by the unique properties of deformable, lightweight, and large area electronics on flexible substrates [2], which are relevant for applications

Submitted for review xxxxxx 2023. This work was partially funded by the Autonomous Province of Bozen-Bolzano-South Tyrol’s European Regional Development Fund (ERDF): project code EFRE/FESR 1140-PhyLab; in part by the International Joint Cooperation South Tyrol-Switzerland Swiss National Foundation (SNF) FLEXIBOTS project grant: 2/34; in part by the Deutsche Forschungsgemeinschaft (DFG) FFlexCom Initiative through the Project WISDOM II grant: 271795180 in part by ministerial funds foreseen by DM 1061/2021:NOP “Research and Innovation” 2014-2020 Action IV.4 “PhDs and research contracts on innovation issues. (Corresponding authors: Giuseppe Cantarella, and Qazi Zahid Husain.)

Koichi Ishida, Tilo Meister, and Frank Ellinger are with the Chair of Circuit Design and Network Theory, Technische Universität Dresden (TU Dresden), 01069 Dresden, Germany.

Qazi Zahid Husain, Dianne Corsino, Federica Catania, and Niko Münzenrieder are with the Faculty of Engineering, Free University of Bozen-Bolzano, 39100 Bozen-Bolzano, Italy (email:qhusain@unibz.it).

Giuseppe Cantarella is with the Department of Physics, Informatics and Mathematics, Università degli Studi di Modena e Reggio Emilia, 341121 Modena, Italy (email:giuseppe.cantarella@unimore.it).

This is the author’s version of the article, which has not been fully edited and content may differ from the final publication.

© 2024 The Authors. This work is licensed under a Creative Commons Attribution-NonCommercial-NoDerivatives 4.0 License.

For more information, see <https://creativecommons.org/licenses/by-nc-nd/4.0/>

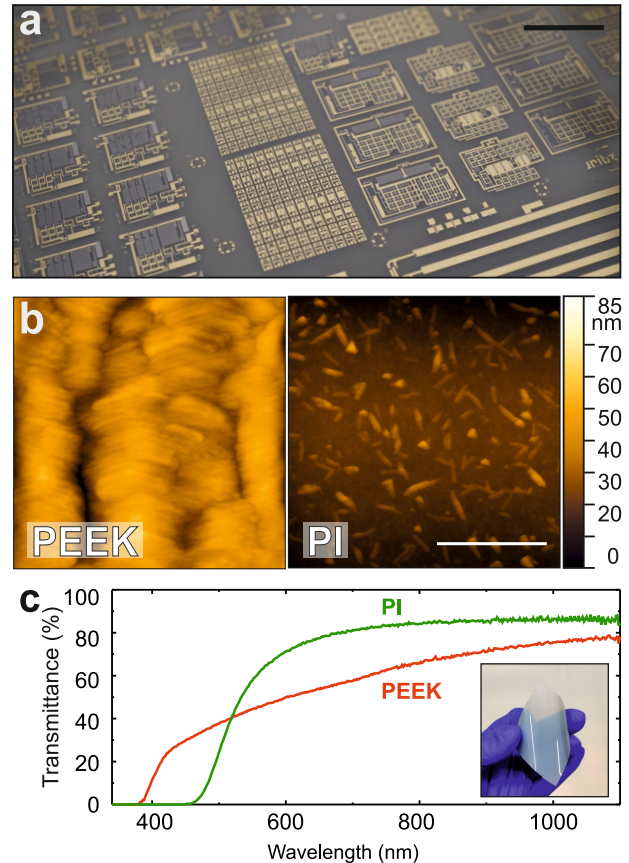


Fig. 1. Thin-film electronics on a flexible PEEK substrate. a) Image of a fully processed PEEK substrate (Scale bar: 5 mm) b) AFM image (Scale bar: 1 μm) and c) optical transmittance of PEEK and PI foils, and image inset illustrating the transparency of the PEEK foil.

such as flexible display [3], soft robotics [4], sensor systems [5], and integrated circuits [6], [7]. Such applications have been made possible by progress in materials science enabling the fabrication of more and more advanced flexible devices. Here, the employment of advanced substrates, combining mechanical flexibility and stability with sufficient chemical and thermal resistance, is a key aspect. A variety of substrates including polyethylene naphthalate (PEN) [8], polyethylene terephthalate (PET) [9], polyimide (PI) [10], metal foil [11], paper [12], or flexible glass [13] are used. In this regards, a possible alternative is polyetheretherketone (PEEK), which is a semi-crystalline thermoplastic that exhibits outstanding

The DOI of the final version is 10.1109/TED.2024.3453220

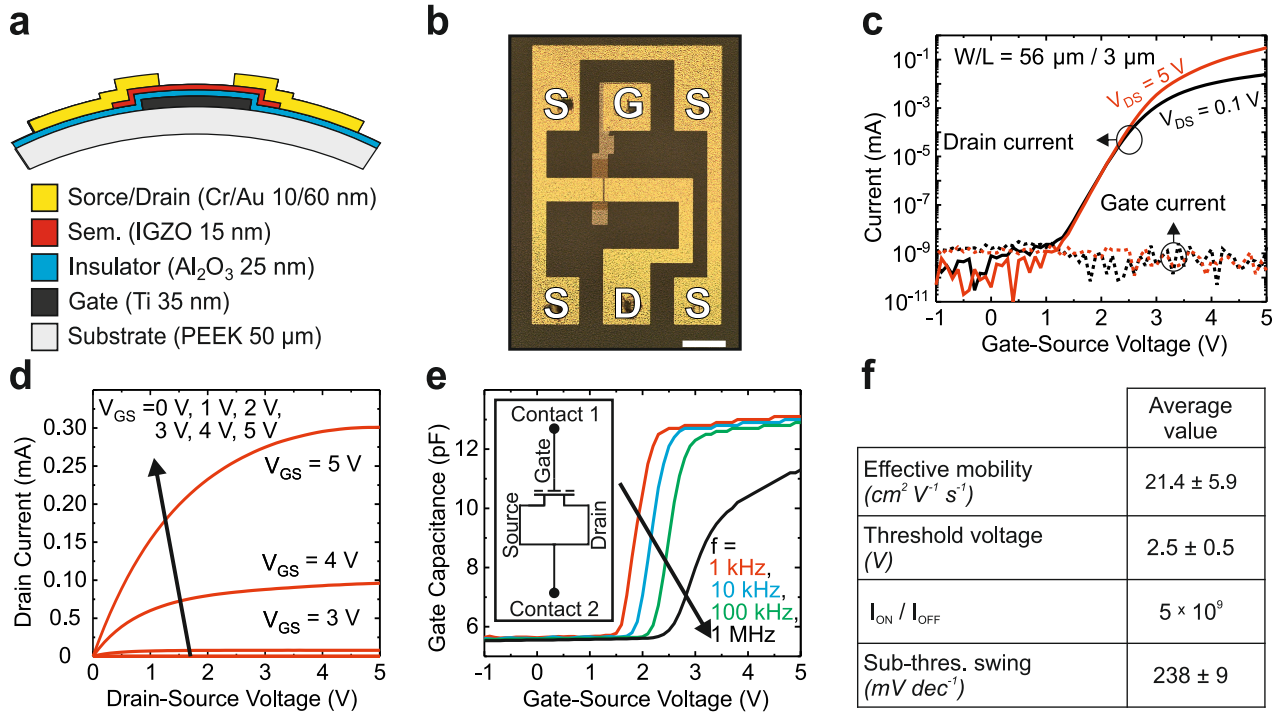


Fig. 2. Fabrication and DC performance of IGZO TFTs on PEEK. a) Schematic cross-section. b) Micrograph of an individual TFT (Scale bar: $100 \mu\text{m}$, G =gate, S =source, and D =drain). c) Transfer, d) output, and e) frequency-dependent capacitance-voltage characteristics of a TFT with W/L ratio: $56 \mu\text{m} / 3 \mu\text{m}$. f) Average and standard deviation performance parameters of all measured nine TFTs.

mechanical and chemical properties, high thermal stability, and low friction coefficient [14], [15]. This thermoplastic is extremely valuable thanks to its bone-like elastic modulus [16], radiolucency [17], and biocompatibility [18]. Furthermore, it was approved as a medical-grade material by the Food and Drug Administration (FDA) in the late 1990s, and recently studied and used as a substitute for metallic implant materials [19], showing its potential for flexible and implantable electronics. In addition, PEEK is biocompatible and recyclable [20], [21], helping the reduction of plastic waste, as reported in the United Nations (UN) Agenda 2030 for Sustainable Development [22]. In parallel, different Thin-Film Transistor (TFT) technologies have been investigated. Among the various semiconductors, such as organics [23], non-crystalline silicon [24], poly-crystalline silicon [25], or 2D-materials [26], metal oxide semiconductors and in particular amorphous InGaZnO (IGZO) [27], offer good electrical properties, large-area uniformity, better transparency, and low-temperature processability [28].

Here, the fabrication of IGZO-based TFTs directly on this biocompatible foil is demonstrated. Although IGZO-based TFTs fabricated on PEEK are presented [29], no comprehensive discussion is reported on these devices' electrical, mechanical, and reliability performance. Both AC and DC performances are reported, resulting in effective mobility μ_{eff} of $19.6 \text{ cm}^2 \text{V}^{-1} \text{s}^{-1}$, a threshold voltage V_{TH} of 2.9 V , unity gain frequency of current gain h_{21} of 5.4 MHz , unity gain frequency of maximum stable gain (MSG) of 28.5 MHz . Bias stress tests as well as static and dynamic bending experiments are performed, proving TFT functionality down to 3 mm bending radius and after five thousand cycles.

II. FABRICATION

The fully processed substrate is shown in Fig. 1a. Bottom-gate inverted-staggered IGZO TFTs were fabricated on a $7 \text{ cm} \times 7 \text{ cm}$ large and $50 \mu\text{m}$ thick flexible PEEK (BIEGLO GmbH) foil. In order to investigate the suitability of PEEK as a polymeric substrate for device fabrication, AFM measurements were performed. The surface roughness of the PEEK foil was measured to be 8.2 nm , which is comparable to that of polyimide (Kapton), with a roughness of 5.6 nm , as shown in Fig. 1b, encouraging the employment of PEEK as carrier substrate for thin-film electronics. Additionally, optical measurements were conducted to assess the transmittance of the PEEK foil. The transmittance value was calculated by taking the average value of the transmittance in the visible and near-infrared wavelength region ($450 \text{ nm} - 900 \text{ nm}$) [30]. The transmittance of the PEEK foil resulted in an average value of 55% , which is close to the transmittance of 67% observed for the polyimide foil (see Fig. 1c). The fabrication was performed on a free-standing substrate using standard UV lithography. First, the substrate was cleaned in acetone and isopropanol for 5 min each. The substrate was then dried in an oven at 200°C for 24 h . A 35 nm thick Ti gate layer was deposited by e-beam evaporation (Plassys) and structured by lift-off. Afterwards, a 25 nm Al_2O_3 gate insulating layer was grown by atomic layer deposition (Picosun Sunale R-150B) using a deposition temperature of 150°C . This was the highest temperature used during the fabrication process. Next, a 15 nm thick IGZO layer was deposited by room temperature RF magnetron sputtering using a ceramic target with atomic composition of In:Ga:Zn:O = 1:1:1:4 (PVD system). Both

Al_2O_3 and IGZO were individually structured by wet etching. The fabrication process was concluded by the deposition of source and drain contacts utilizing 10 nm/60 nm of e-beam evaporated Cr/Au patterned by lift-off. A schematic diagram of the cross-section of the IGZO TFTs is shown in Fig. 2a, while micrograph of an individual TFT is shown in Fig. 2b.

III. RESULTS AND DISCUSSION

A total of 18 TFTs with different channel width (W) over length (L) ratios were characterised. The measurements were all done in a standard lab, and the Shichman-Hodges model was used to get all the performance parameters from TFTs in the saturation regime [31].

A. DC performance

DC characteristics of TFTs with nine different channel width (W) over length (L) ratios ranging from $56\ \mu\text{m}/3\ \mu\text{m}$ to $315\ \mu\text{m}/111\ \mu\text{m}$ were measured using a Keysight B1500A parameter analyzer. Representative transfer and output characteristics of a TFT with $3\ \mu\text{m}$ channel length are shown in Figs. 2c and 2d. The TFT exhibits an effective mobility μ_{eff} of $19.6\ \text{cm}^2\ \text{V}^{-1}\ \text{s}^{-1}$, an on-off current ratio I_{ON}/I_{OFF} of 3×10^{10} , a threshold voltage V_{TH} of 2.9 V, and a subthreshold swing SS of $233\ \text{mVdec}^{-1}$. At the same time, the gate leakage current is always smaller than $10^{-12}\ \text{A}$. The corresponding average values and standard deviations for all measured TFTs are summarised in Fig. 2e. These values result in a maximum transconductance g_m of 0.62 mS for the $3\ \mu\text{m}$ long TFT and are comparable to other flexible IGZO TFTs fabricated on more conventional polymer substrates [32].

Additionally, the gate capacitance was measured for different frequencies (all within the operational range of the device) and gate bias voltages while the source and drain contacts were grounded. A representative measurement is shown in Fig. 2f. A TFT with $3\ \mu\text{m}$ channel length and overlaps between gate and source-drain contacts of $36\ \mu\text{m}$, exhibits a low-frequency total gate capacitance C_G of 13.2 pF and a total overlap capacitance (measured while the transistor is off) of 5.5 pF. The average resulting specific gate oxide capacitance is $3.4\ \text{mF m}^{-2}$. Furthermore, the measurement illustrates the frequency dependency of the channel capacitance, typical for TFT with the employed geometry [33].

B. Reliability performance

To evaluate the electrical stability of the TFTs fabricated on the PEEK substrate, positive bias stress (PBS) and negative bias stress (NBS) tests of TFTs with 6 different W/L ratios ranging from $315\ \mu\text{m}/5\ \mu\text{m}$ to $315\ \mu\text{m}/82\ \mu\text{m}$ were carried out at room temperature. Gate voltages of $\pm 1.25\ \text{V}$, $\pm 2.5\ \text{V}$, and $\pm 5\ \text{V}$ are applied for 60 s, 120 s, 300 s, and 600 s, while the drain and source terminal is grounded. For every measurement, a new TFT was used. After every stress duration transfer and output characteristics are measured, as shown in Figs. 3a-b and Figs. 3d-e. A gate voltage of $+5\ \text{V}$ leads to a maximum variation in V_{TH} , μ_{eff} , and SS of $+0.3\ \text{V}$, $+18\%$, and $+11.7\%$, respectively. As shown in Fig. 3c positive trends

are obtained in the V_{TH} shift during the PBS test because of the charge trapping between the active and dielectric layer or formation of defects in active channel layers [34]. After applying $-5\ \text{V}$ gate voltage, maximum deviation in V_{TH} , μ_{eff} are reported $-0.6\ \text{V}$, -21% , respectively. The significant change in SS , are observed $+38.5\%$. For the NBS, negative trends are attained in the threshold voltage shift in Fig. 3f. The free electrons created in the active layer during an extended period of stress time are the cause for the negative V_{TH} shift.

C. AC performance

The TFTs AC performance can be estimated by the transit frequency f_T , based on the following ideal equation [35]:

$$f_t = \frac{g_m}{2\pi C_G} \quad (1)$$

However, here the AC performance was also directly measured by acquiring the TFT's S-parameters using a Keysight E5061B ENA network analyzer. To ensure reliable measurements Ground-Signal-Ground (GSG) RF probes, matching the GSG layout of the TFTs were used. Fig. 4a shows the S-parameters of a $3\ \mu\text{m}$ long TFT biased at $V_{DS} = V_{GS} = 5\ \text{V}$. The S-parameters are used to calculate the current gain h_{21} (Fig. 4b), which in turn can be used to experimentally determine f_T as the unity gain frequency of h_{21} . The measured value of f_T is 5.4 MHz, which is close the 7.5 MHz estimated using Equation 1. Additionally, the S-parameters are also used to calculate the maximum stable gain MSG (Fig. 4c). These are used to determine f_{max} as the maximum frequency at which the TFT can provide power gain. The resulting f_{max} value, extracted from MSG is 28.5 MHz. The found f_T and f_{max} frequencies are in line with the performance of other flexible IGZO TFTs [30], and illustrate that these devices can be used for the realization of analog circuits.

D. Static Bending performance

To evaluate the mechanical performance of the TFTs on PEEK substrates, DC measurements were performed while the substrate was subsequently wrapped around cylindrical rods with different radii (15 mm, 5 mm, 4 mm, and 3 mm). This induced tensile mechanical strain up to 0.8% parallel to the TFT channels calculated according to [36]. The device (W/L = $56\ \mu\text{m}/7.5\ \mu\text{m}$) stayed fully functional while being bent and re-flattened (shown in Fig. 5). Here a bending radius of 3 mm induced the largest parameter shifts, which were $+0.4\%$ in μ_{eff} , $-0.2\ \text{V}$ in V_{TH} , and $+5.9\%$ in SS . At the same time, radii below 3 mm caused permanent failure due to the formation of cracks. The variations in the bending performance are in the same order of magnitude as those seen with other flexible substrates [37], this is attributed to the elastic modulus, and Vickers microhardness of pure PEEK reaching values of 3.9 GPa and 21.7 GPa, respectively [38].

E. Dynamic bending performance

The mechanical stability of the TFTs was further investigated by dynamic bending test of the devices. The TFT

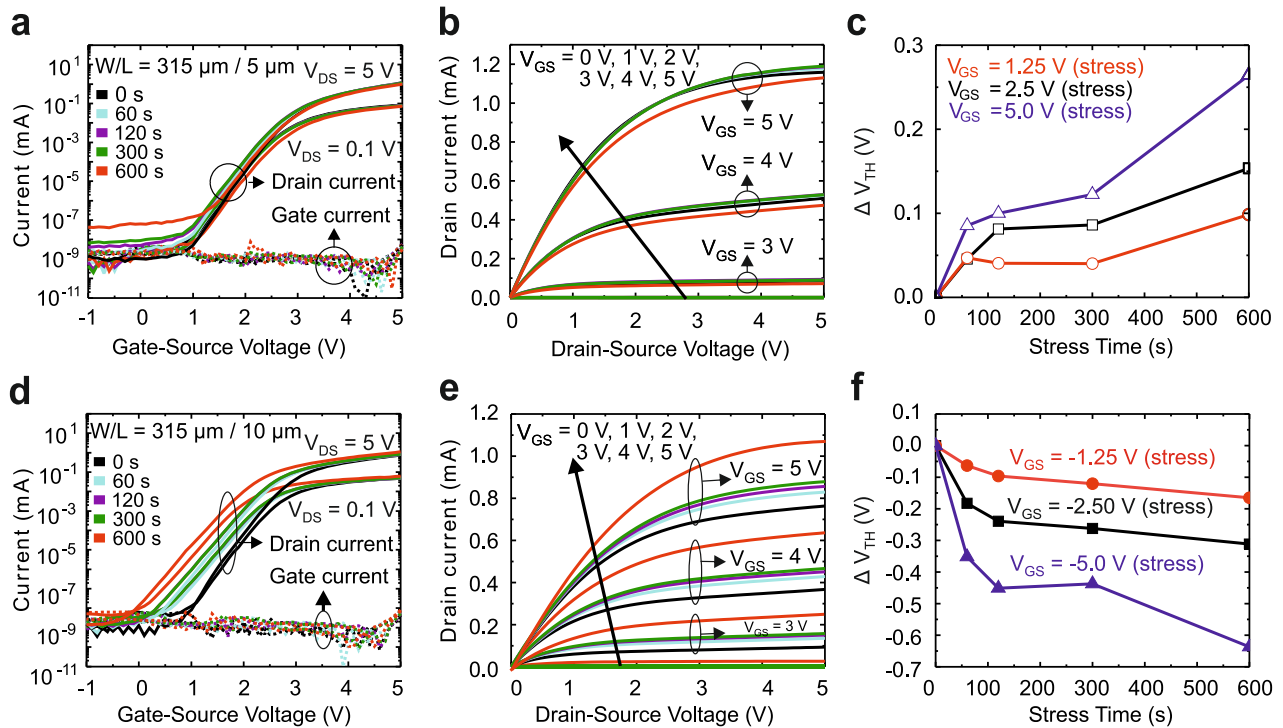


Fig. 3. Reliability performance: Representative evolution of (a) transfer and (b) output characteristics of the IGZO TFTs subjected to a positive gate voltage stress. (c) Summary of threshold voltage shift as a function of time at different positive gate voltage stress. (d) Transfer and (e) output characteristics of the IGZO TFTs subjected to a negative gate voltage stress. (f) Summary of threshold voltage shift as a function of time at different negative gate voltage stress.

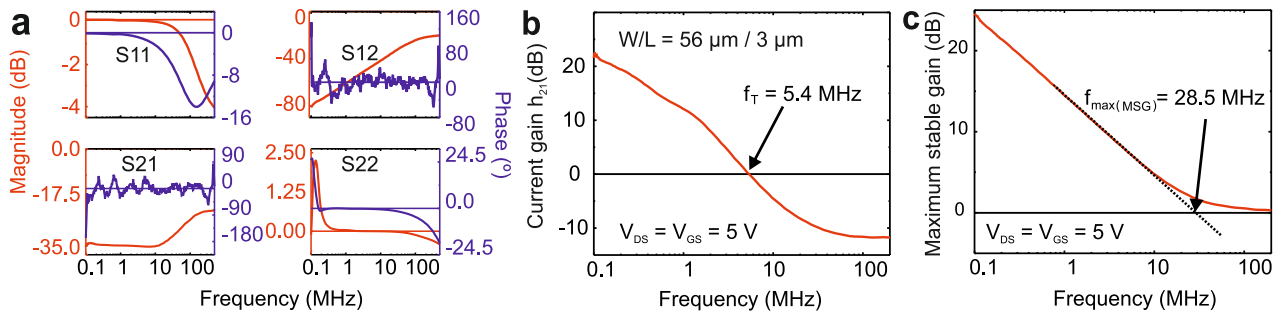


Fig. 4. AC performance: a) S-parameter measurements, b) Absolute value of current gain, and c) Maximum stable gain for different frequencies.

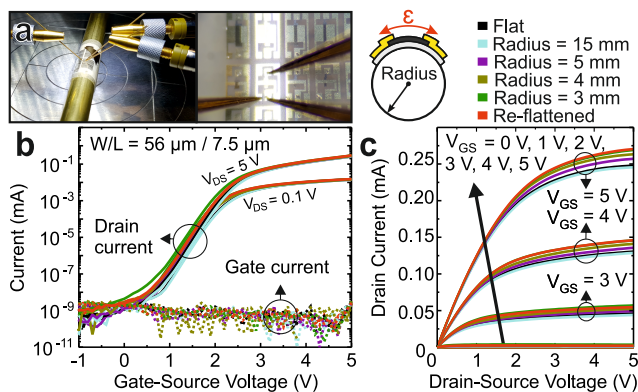


Fig. 5. Static bending performance. a) Images of bent substrate and contacted TFTs. b) Transfer characteristics and c) output characteristics of IGZO TFTs on PEEK measured at different bending radii down to 3 mm and after being re-flattened.

is adhered onto a strip with the help of polyester double-sided tape (3M 93010LE) that is clamped on both ends. One end is then allowed to move back and forth where the device is repeatedly bent down to a radius of 20 mm and re-flattened. The transfer and output characteristics of the TFTs were measured after bending for 100 cycles, 500 cycles, 1000 cycles, and 5000 cycles, as shown in Figs. 6a and 6b. Maximum shifts in the μ_{eff} and V_{TH} were obtained at 5000 bending cycles of +12.9%, and +0.2 V as represented in Fig. 6c. A similar variation in the μ_{eff} and V_{TH} was reported in [39], [40]. These results validate the mechanical stability of the devices on PEEK.

IV. CONCLUSION

Flexible IGZO-based TFTs are demonstrated on PEEK foil. The devices exhibit state-of-the-art DC and AC performance, including I_{ON}/I_{OFF} ratio exceeding 10^{10} , and a maximum

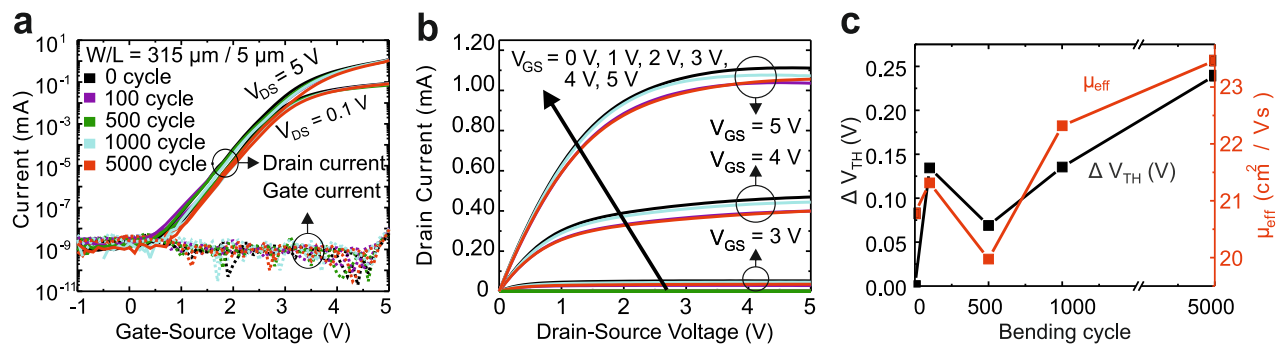


Fig. 6. Dynamic bending performance: Variations in the (a) transfer and (b) output characteristics, and (c) summary of changes in the mobility and threshold voltage shift versus the number of bending.

oscillation frequency of 28.5 MHz. After applying +5 V bias stress for 5 min, the maximum variation in the V_{TH} observed is +0.3 V, when -5 V bias stress is applied, a maximum deviation in the V_{TH} -0.6 V is found, which confirms the electrical stability of the TFTs. The device functionality is demonstrated down to a tensile bending radius of 3 mm. In addition, after undergoing 5000 cycles of dynamic bending with a radius of curvature of 20 mm, the device demonstrated +0.2 V variation in V_{TH} which confirmed the outstanding mechanical durability of the TFTs. Considering the desirable properties of PEEK, including biocompatibility, and flexibility, as a substrate for flexible electronics, this work represents a first step towards the implementation of polyetheretherketone in applications, such as biomedicine, wearable electronics, or soft robotics. Taking advantage of the compatibility of PEEK foils with thin-film processing and its transmittance comparable to widely employed flexible substrates, future works will be devoted to the realization of self-aligned TFTs on this substrate, aiming at flexible devices with channel length below 1 μm .

REFERENCES

- [1] T. P. Brody, "The thin film transistor—a late flowering bloom," *IEEE Transactions on Electron Devices*, vol. 31, no. 11, pp. 1614–1628, Nov. 1984. [Online]. Available: <https://doi.org/10.1109/T-ED.1984.21762>
- [2] A. Nathan, A. Ahnood, M. T. Cole, S. Lee, Y. Suzuki, P. Hiralal, F. Bonaccorso, T. Hasan, L. Garcia-Gancedo, A. Dyadyusha, S. Haque, P. Andrew, S. Hofmann, J. Moultrie, D. Chu, A. J. Flewitt, A. C. Ferrari, M. J. Kelly, J. Robertson, G. A. J. Amaratunga, and W. I. Milne, "Flexible electronics: the next ubiquitous platform," *Proceedings of the IEEE*, vol. 100, no. Special Centennial Issue, pp. 1486–1517, May 2012. [Online]. Available: <https://doi.org/10.1109/JPROC.2012.2190168>
- [3] P. Mach, S. Rodriguez, R. Nortrup, P. Wiltzius, and J. A. Rogers, "Monolithically integrated, flexible display of polymer-dispersed liquid crystal driven by rubber-stamped organic thin-film transistors," *Applied Physics Letters*, vol. 78, no. 23, pp. 3592–3594, Jun. 2001. [Online]. Available: <https://doi.org/10.1063/1.1377312>
- [4] A. Marette, A. Poulin, N. Besse, S. Rosset, D. Briand, and H. Shea, "Flexible zinc-tin oxide thin film transistors operating at 1 kv for integrated switching of dielectric elastomer actuators arrays," *Advanced materials*, vol. 29, no. 30, Aug. 2017, Art. no. 1700880. [Online]. Available: <https://doi.org/10.1002/adma.201700880>
- [5] J. C. Costa, F. Spina, P. Lugoda, L. Garcia-Garcia, D. Roggen, and N. Müntenrieder, "Flexible sensors—from materials to applications," *Technologies*, vol. 7, no. 2, Apr. 2019, Art. no. 35. [Online]. Available: <https://doi.org/10.3390/technologies7020035>
- [6] Z. You, H. Liu, Y. Xu, Z. Ma, and G. Qin, "A flexible monolithic integrated silicon low noise amplifier on plastic substrate," *Journal of Physics D: Applied Physics*, vol. 54, no. 11, Jan. 2021, Art. no. 11LT01. [Online]. Available: <https://doi.org/10.1088/1361-6463/abd05f>
- [7] J. Biggs, J. Myers, J. Kufel, E. Ozer, S. Craske, A. Sou, C. Ramsdale, K. Williamson, R. Price, and S. White, "A natively flexible 32-bit Arm microprocessor," *Nature*, vol. 595, no. 7868, pp. 532–536, Jul. 2021. [Online]. Available: <https://doi.org/10.1038/s41586-021-03625-w>
- [8] C. Sheraw, L. Zhou, J. Huang, D. Gundlach, T. Jackson, M. Kane, I. Hill, M. Hammond, J. Campi, B. Greening, J. Francl, and J. West, "Organic thin-film transistor-driven polymer-dispersed liquid crystal displays on flexible polymeric substrates," *Applied physics letters*, vol. 80, no. 6, pp. 1088–1090, Feb. 2002. [Online]. Available: <https://doi.org/10.1063/1.1448659>
- [9] S. Das, R. Gulotty, A. V. Sumant, and A. Roelofs, "All two-dimensional, flexible, transparent, and thinnest thin film transistor," *Nano letters*, vol. 14, no. 5, pp. 2861–2866, Apr. 2014. [Online]. Available: <https://doi.org/10.1021/nl5009037>
- [10] G. Cantarella, J. Costa, T. Meister, K. Ishida, C. Carta, F. Ellinger, P. Lugli, N. Müntenrieder, and L. Petti, "Review of recent trends in flexible metal oxide thin-film transistors for analog applications," *Flexible Printed Electron.*, vol. 5, no. 3, Aug. 2020, Art. no. 033001. [Online]. Available: <https://doi.org/10.1088/2058-8585/aba79a>
- [11] T. Afentakis, M. Hatalis, A. T. Voutsas, and J. Hartzell, "Design and fabrication of high-performance polycrystalline silicon thin-film transistor circuits on flexible steel foils," *IEEE transactions on electron devices*, vol. 53, no. 4, pp. 815–822, Apr. 2006. [Online]. Available: <https://doi.org/10.1109/TED.2006.871174>
- [12] F. Eder, H. Klauk, M. Halik, U. Zschieschang, G. Schmid, and C. Dehm, "Organic electronics on paper," *Applied Physics Letters*, vol. 84, no. 14, pp. 2673–2675, Apr. 2004. [Online]. Available: <https://doi.org/10.1063/1.1690870>
- [13] C. H. Lee, J.-H. Kim, C. Zou, I. S. Cho, J. M. Weisse, W. Nemeth, Q. Wang, A. C. Van Duin, T.-S. Kim, and X. Zheng, "Peel-and-stick: mechanism study for efficient fabrication of flexible/transparent thin-film electronics," *Scientific reports*, vol. 3, no. 1, pp. 1–6, Oct. 2013. [Online]. Available: <https://doi.org/10.1038/srep02917>
- [14] S. M. Kurtz, *PEEK biomaterials handbook*. William Andrew, Mar. 2019. [Online]. Available: <https://doi.org/10.1016/B978-0-12-812524-3.00001-6>
- [15] S. Kurtz, "Chemical and radiation stability of peek," *PEEK Biomaterials Handbook*, pp. 75–79, Dec. 2012. [Online]. Available: <https://doi.org/10.1016/B978-1-4377-4463-7.10006-5>
- [16] E. Alexakou, M. Damanaki, P. Zoidis, E. Bakiri, N. Mouzis, G. Smidt, and S. Kourtis, "Peek high performance polymers: A review of properties and clinical applications in prosthodontics and restorative dentistry," *Eur. J. Prosthodont. Restor. Dent.*, vol. 27, pp. 113–121, 2019. [Online]. Available: <https://doi.org/10.1922/EJPRD-0189Zzoidis09>
- [17] D. Almasi, N. Iqbal, M. Sadeghi, I. Sudin, M. R. Abdul Kadir, T. Kamarul *et al.*, "Preparation methods for improving peek's bioactivity for orthopedic and dental application: a review," *International journal of biomaterials*, vol. 2016, 2016. [Online]. Available: <https://doi.org/10.1155/2016/8202653>
- [18] J. M. Toth, "Biocompatibility of peek polymers," in *PEEK biomaterials handbook*. Elsevier, 2019, pp. 107–119. [Online]. Available: <https://doi.org/10.1016/B978-0-12-812524-3.00008-9>
- [19] C.-M. Han, E.-J. Lee, H.-E. Kim, Y.-H. Koh, K. N. Kim, Y. Ha, and S.-U. Kuh, "The electron beam deposition of titanium on polyetheretherketone (peek) and the resulting enhanced biological properties," *Biomaterials*, vol. 31, no. 13, pp. 3465–3470, May 2010. [Online]. Available: <https://doi.org/10.1016/j.biomaterials.2009.12.030>

- [20] A. Mclauchlin, O. Ghita, and L. Savage, "Studies on the reprocessability of poly(ether ether ketone) (peek)," *Journal of Materials Processing Technology*, vol. 214, pp. 75–80, Jan. 2014. [Online]. Available: <https://doi.org/10.1016/j.jmatprotec.2013.07.010>
- [21] J. Xu, Z. Zhang, X. Xiong, and H. Zeng, "A new solvent for poly (ether ether ketone)," *Polymer*, vol. 33, no. 20, pp. 4432–4434, Mar. 1992. [Online]. Available: [https://doi.org/10.1016/0032-3861\(92\)90293-6](https://doi.org/10.1016/0032-3861(92)90293-6)
- [22] G. Halkos and E.-C. Gkampoura, "Where do we stand on the 17 sustainable development goals? an overview on progress," *Economic Analysis and Policy*, vol. 70, pp. 94–122, Jun. 2021. [Online]. Available: <https://doi.org/10.1016/j.eap.2021.02.001>
- [23] Y.-Y. Lin, D. Gundlach, S. F. Nelson, and T. N. Jackson, "Pentacene-based organic thin-film transistors," *IEEE Transactions on Electron Devices*, vol. 44, no. 8, pp. 1325–1331, Aug. 1997. [Online]. Available: <https://doi.org/10.1109/16.605476>
- [24] K. H. Cherenack, A. Z. Kattamis, B. Hekmatshoar, J. C. Sturm, and S. Wagner, "Amorphous-silicon thin-film transistors fabricated at 300°C on a free-standing foil substrate of clear plastic," *IEEE electron device letters*, vol. 28, no. 11, pp. 1004–1006, Nov. 2007. [Online]. Available: <https://doi.org/10.1109/LED.2007.907411>
- [25] T.-C. Chang, Y.-C. Tsao, P.-H. Chen, M.-C. Tai, S.-P. Huang, W.-C. Su, and G.-F. Chen, "Flexible low-temperature polycrystalline silicon thin-film transistors," *Materials Today Advances*, vol. 5, Mar. 2020, Art. no. 100040. [Online]. Available: <https://doi.org/10.1016/j.mtadv.2019.100040>
- [26] Q. He, Z. Zeng, Z. Yin, H. Li, S. Wu, X. Huang, and H. Zhang, "Fabrication of flexible mos2 thin-film transistor arrays for practical gas-sensing applications," *Small*, vol. 8, no. 19, pp. 2994–2999, Oct. 2012. [Online]. Available: <https://doi.org/10.1002/sml.201201224>
- [27] K. Nomura, H. Ohta, A. Takagi, T. Kamiya, M. Hirano, and H. Hosono, "Room-temperature fabrication of transparent flexible thin-film transistors using amorphous oxide semiconductors," *Nature*, vol. 432, no. 7016, pp. 488–492, Nov. 2004. [Online]. Available: <https://doi.org/10.1038/nature03090>
- [28] K. Nomura, A. Takagi, T. Kamiya, H. Ohta, M. Hirano, and H. Hosono, "Amorphous oxide semiconductors for high-performance flexible thin-film transistors," *Jpn J Appl Phys*, vol. 45, no. 5, pp. 4303–4308, Apr. 2006. [Online]. Available: <https://doi.org/10.1143/JJAP.45.4303>
- [29] F. Li, E. Smits, L. Leuken, d. Haas, T. Ellis, J.-L. Steen, A. Tripathi, K. Myny, M. Ameys, S. Schols, P. Heremans, and G. Gelinck, "32.2: Invited paper: Integration of flexible amoled displays using oxide semiconductor tft backplanes," in *SID Symposium Digest of Technical Papers*, vol. 45, no. 1. Wiley Online Library, Jun. 2014, pp. 431–434. [Online]. Available: <https://doi.org/10.1002/j.2168-0159.2014.tb00116.x>
- [30] F. Catania, M. Ahmad, D. Corsino, N. S. Khaanghah, L. Petti, N. Münzenrieder, and G. Cantarella, "Ac performance of flexible transparent ingazno thin-film transistors and circuits," *IEEE Transactions on Electron Devices*, vol. 69, no. 9, pp. 4930–4935, Sep. 2022. [Online]. Available: <https://doi.org/10.1109/TED.2022.3193012>
- [31] H. Shichman and D. A. Hodges, "Modeling and simulation of insulated-gate field-effect transistor switching circuits," *IEEE Journal of Solid-State Circuits*, vol. 3, no. 3, pp. 285–289, Sep. 1968. [Online]. Available: <https://doi.org/10.1109/JSSC.1968.1049902>
- [32] L. Petti, N. Münzenrieder, C. Vogt, H. Faber, L. Büthe, G. Cantarella, F. Bottacchi, T. D. Anthopoulos, and G. Tröster, "Metal oxide semiconductor thin-film transistors for flexible electronics," *Applied Physics Reviews*, vol. 3, no. 2, Jun. 2016, Art. no. 021303. [Online]. Available: <https://doi.org/10.1063/1.4953034>
- [33] N. Münzenrieder, L. Petti, C. Zysset, T. Kinkeldei, G. A. Salvatore, and G. Tröster, "Flexible self-aligned amorphous InGaZnO thin-film transistors with submicrometer channel length and a transit frequency of 135 MHz," *IEEE Transactions on Electron Devices*, vol. 60, no. 9, pp. 2815–2820, Sep. 2013. [Online]. Available: <https://doi.org/10.1109/TED.2013.2274575>
- [34] E. N. Cho, J. H. Kang, C. E. Kim, P. Moon, and I. Yun, "Analysis of bias stress instability in amorphous ingazno thin-film transistors," *IEEE Transactions on Device and Materials Reliability*, vol. 11, no. 1, pp. 112–117, Mar. 2011. [Online]. Available: <https://doi.org/10.1109/TDMR.2010.2096508>
- [35] N. Münzenrieder, G. A. Salvatore, L. Petti, C. Zysset, L. Büthe, C. Vogt, G. Cantarella, and G. Tröster, "Contact resistance and overlapping capacitance in flexible sub-micron long oxide thin-film transistors for above 100 MHz operation," *Applied Physics Letters*, vol. 105, no. 26, p. Art. no. 263504, Dec. 2014. [Online]. Available: <https://doi.org/10.1063/1.4905015>
- [36] H. Gleskova, S. Wagner, and Z. Suo, "a-si: H thin film transistors after very high strain," *Journal of Non-Crystalline Solids*, vol. 266, pp. 1320–1324, May 2000. [Online]. Available: [https://doi.org/10.1016/S0022-3093\(99\)00944-8](https://doi.org/10.1016/S0022-3093(99)00944-8)
- [37] N. Münzenrieder, C. Zysset, T. Kinkeldei, and G. Tröster, "Design rules for igzo logic gates on plastic foil enabling operation at bending radii of 3.5 mm," *Transactions on Electron Devices, IEEE*, vol. 59, no. 8, pp. 2153–2159, Aug. 2012. [Online]. Available: <https://doi.org/10.1109/TED.2012.2198480>
- [38] M. Kuo, C. Tsai, J. Huang, and M. Chen, "Peek composites reinforced by nano-sized sio2 and al2o3 particulates," *Materials chemistry and physics*, vol. 90, no. 1, pp. 185–195, Mar. 2005. [Online]. Available: <https://doi.org/10.1016/j.matchemphys.2004.10.009>
- [39] N. Münzenrieder, K. Cherenack, and G. Tröster, "The effects of mechanical bending and illumination on the performance of flexible igzo TFTs," *Transactions on Electron Devices, IEEE*, vol. 58, pp. 2041–2048, Jul. 2011. [Online]. Available: <https://doi.org/10.1109/TED.2011.2143416>
- [40] Y. C. Kim, S. J. Lee, I.-K. Oh, S. Seo, H. Kim, and J.-M. Myoung, "Bending stability of flexible amorphous igzo thin film transistors with transparent izo/ag/izo oxide–metal–oxide electrodes," *Journal of Alloys and Compounds*, vol. 688, pp. 1108–1114, Dec. 2016. [Online]. Available: <https://doi.org/10.1016/j.jallcom.2016.07.169>